Copper/Iron Brake Friction for Military Aircraft Application

Thiago Duque Estrada da Silva Santos[1], Inácio Regiani[2], Roberta Jachura Rocha[1], José Atílio Fritz Fidel Rocco[1]

Santos TDES http://orcid.org/0000-0002-1485-5953
Regiani I http://orcid.org/0000-0002-5642-2056
Rocha RJ http://orcid.org/0000-0003-1023-0021
Rocco JAFF http://orcid.org/0000-0002-6004-6997

How to cite:

Santos TDES; Regiani I; Rocha RJ; Rocco JAFF (2018) Copper/Iron Brake Friction for Military Aircraft Application. J Aerosp Technol Manag, 10: e2018. doi: 10.5028/jatm.v10.834.

ABSTRACT: The present study assesses the influence of non-metallic constituents and manufacturing parameters, such as compaction pressure and sintering temperature, to produce a metal matrix composite (MMC) of copper/iron, based on the brake disc of aircraft AT-29 SuperTucano. The samples were produced with six different compositions, by varying the amount of abrasive particles (quartz and zirconia silicate) and the solid lubricant (graphite), with one of the compositions manufactured without the addition of graphite. The compaction pressures were 210 and 420 MPa, with sintering temperatures of 950 °C and 1050 °C in a furnace with controlled atmosphere of argon + 10% H_2. After sintering, the effectiveness of the sintering process was evaluated through the apparent density (Archimedes's method), Brinell and Vickers hardness, and the microstructure by Scanning Electron Microscopy (SEM). The sintering process was severely affected by the solid lubricant (graphite): its reduction resulted in a density increase near 18%, and the hardness of the compound up to 62%. The hardness values demonstrated significant variation with compaction pressure, with a pronounced effect on compounds with less non-metallic elements. SEM analysis demonstrated that not only graphite, but also the ceramic particles affected the sintering process through the agglomeration of inclusions into the metal-metal interface. The samples without graphite exhibited almost the same value of pores after sintering, regardless of the compaction pressure, indicating that the graphite content affects directly the sintering process, regardless of the compaction pressure.

KEYWORDS: Friction, Sintering, Aircraft brakes.

INTRODUCTION

Friction materials formed by sintered metal matrix (MMC) have a variety of constituents such as metals (iron and copper with or without alloying elements), solid lubricants (graphite, lead and MoS_2) and ceramic abrasives (silica, mullite, alumina and silicon carbide), being widely used in aircraft brake systems (German 1998). To ensure the requirements related to the aircraft braking process, the friction material must have a stable and high friction coefficient, low wear rate, mechanical strength at high temperatures and good thermal conductivity (Singaravelu *et al.* 2011).

For having a high thermal conductivity combined with good mechanical resistance, copper is one of the most important components in brake systems, added in the form of powders or fibers (Blau 2001). Iron additions in the copper matrix ensure a greater mechanical strength, thermal stability and reduce the manufacturing cost of the product. The ceramic particles act as abrasives. Its high hardness leads to an increase in mechanical strength and wear resistance of the sintered composite. Recently,

1.Departamento de Ciência e Tecnologia Aeroespacial – Instituto Tecnológico de Aeronáutica – Divisão de Química – São José dos Campos/SP – Brazil.
2.Departamento de Ciência e Tecnologia Aeroespacial – Instituto Tecnológico de Aeronáutica – Divisão de Materiais e Processos – São José dos Campos/SP – Brazil.
Correspondence author: Roberta Jachura Rocha | Departamento de Ciência e Tecnologia Aeroespacial – Instituto Tecnológico de Aeronáutica – Divisão de Química | Praça Mal Eduardo Gomes, 50 | CEP: 12.228-900 – São José dos Campos/SP – Brazil | E-mail: robertarj@gmail.com
Received: Jul. 11, 2016 | **Accepted:** Jun. 29, 2017
Section Editor: José Maria Ferreira

studies (Shabani *et al.* 2016; Cho *et al.* 2008) have shown that zirconium silicate ($ZrSiO_4$) caused considerable increase of the friction coefficient relative to other ceramics used in friction materials such as SiC and SiO_2. The addition of solid lubricants such as graphite and MoS_2 stabilizes friction coefficient and reduces wear (Upadhyaya 2000).

However, the addition of non-metallic particles affects directly the sintering and densification process. Leon *et al.* (2009) analyzed the compressibility behavior of metal-ceramic powders in the preparation of copper base hybrid materials: the higher the ceramic content, the lower the densification obtained regardless of the applied method. Olmos *et al.* (2009) investigated the sintering behavior of metallic copper powder mixed with ceramic inclusions. The addition of inert inclusion (ceramic particles) consistently results in lower densification.

Details and functions of the constituents are determined mostly on experience, empirical observation and trial and error method for new formulations, given the difficulty in obtaining information due to patent issues (Kim *et al.* 2011; Liew and Nirmal 2013). Only a limited number of studies have been reported for sintered compounds with a focus on high-energy brake systems as observed in aircrafts. In addition, the composition of each aircraft friction material is unique, such as the powder metallurgy process for synthesizing the material (Jang and Kim 2000).

The present study assesses the effects of manufacturing parameters, such as the compaction pressure, sintering temperature, and influence of non-metallic constituents in the sintering process and mechanical strength of the compound. The compounds developed have a Cu-Fe matrix, with the addition of $ZrSiO_4$ and SiO_2 as abrasives, and graphite as solid lubricant.

MATERIALS AND METHODOLOGY

Minasolo and Höganäs donated the powders used as raw materials: pure copper, pure iron, quartz (SiO_2), zircon silicate ($ZrSiO_4$), and graphite.

For the analysis of grain size and particles morphology, it was used images obtained by SEM following the ASTM E175-82 and ASTM E766-98 standards. Verification of the powders composition in order to evaluate purity and presence of possible contaminants was performed by XRD and XRF.

The samples were produced with six different compositions, by varying the amount of abrasive particles (quartz and zirconia silicate) and the solid lubricant (graphite), with one of the compositions manufactured without the addition of graphite. Table 1 demonstrates the compositions obtained after the mixtures.

Table 1. Mixtures composition of the samples (values in wt.%).

Sample	Cu	Fe	Graphite	SiO_2	$ZrSiO_4$	Type
I	52	34	8	6	0	↑ Graphite. ↑SiO_2
II	52	34	8	4	2	↑Graphite. SiO_2 + $ZrSiO_4$
III	54.1	35.4	4	4.3	2.2	≈ Graphite. SiO_2 + $ZrSiO_4$
IV	55.8	36.5	1	4.4	2.3	↓ Graphite. SiO_2 + $ZrSiO_4$
V	56.8	37.2	4	1	1	≈ Graphite. ↑ (SiO_2 + $ZrSiO_4$)
VI	59.5	38.5	0	1	1	↓ (SiO_2 + $ZrSiO_4$)

POWDER PROCESSING

The powders mixture was performed in a mixing mill MARCONI MA500 with a fixed speed of approximately 200 RPM during 2 h. Due to the small quantities of each powder mixture (100 g) and the larger size of the disposable container, the mixture was placed in a small plastic container, which rotated inside the larger mill container.

For the composite formation, mixtures were uni-axially compacted in a metallic mold to form cylindrical discs with 15 mm diameter and 7 mm height (Fig. 1). Two different pressing loads were applied for powder compaction: 420 and 210 Mpa. The

pressing loads were defined according to values reported in the literature for metal matrix composite of copper and iron (Nair *et al.* 1993; German 1998; Upadhyaya 2000; Olmos *et al.* 2009). To reduce frictional losses during compaction, zinc stearate was added to the die wall.

Figure 1. Samples after compaction.

The sintering process (Fig. 2) was conducted at two different temperatures, 950 °C and 1050 °C, in a tubular furnace with controlled atmosphere (argon + 10% H_2). The sintering process can be divided into three different phases: pre-sintering, sintering and cooling. The process had a total duration of 112 min. In the pre-sintering phase, the samples were kept for 20 min at a temperature of 600 °C to burn the lubricant used in the compaction die and any other contaminant. Temperature was gradually raised to the sintering temperature over 15 min. Then, the samples were held at that temperature for 50 min. Finally, the cooling was carried out inside the furnace until room temperature.

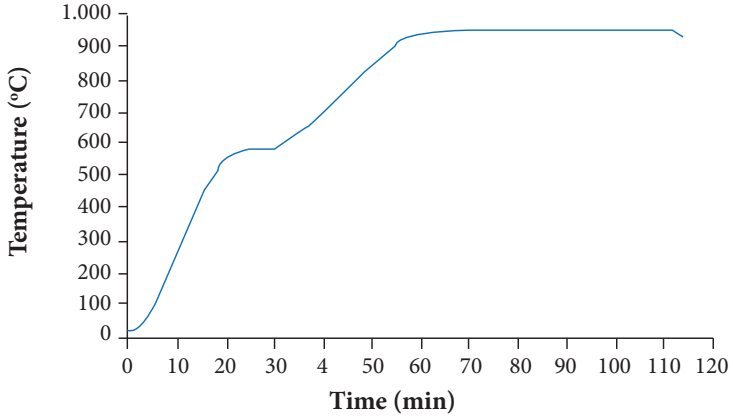

Figure 2. Sintering process.

COMPOSITE EVALUATION

Sintered densities of composites were determined by Archimedes's method using distilled water at 23 °C. Most studies related to the development of friction materials use tests that evaluate the surface hardness of the sample, such as the Vickers hardness test (Leon *et al.* 2009; Shabani *et al.* 2016) or the Brinell hardness test (Moustafa *et al.* 2002; Prabhu 2015) with a smaller diameter ball and lower loading. Therefore, for the purpose of comparison and a pre-evaluation of the compound's performance in future tribological tests, the mechanical behavior and effectiveness of the sintering process was studied by measuring Vickers and Brinell hardness.

Values of Vickers hardness, also referred to as a *micro-hardness* test method, were calculated as the average of five readings for each sample. The Brinell hardness was held in a universal testing machine EMIC with capacity of 20 kN using a load of 500 kg

and a steel sphere with 10 mm diameter as indenter according to ASTM E10. Given the sample size (cylindrical with 15 mm diameter), the sphere with 10 mm diameter scans a large area on the sample even in terms of the indentation depth, thus providing the possibility to indirectly evaluate how the constituents (composition) and parameters process influenced on sintering.

The microstructures of the sintered composites were studied by scanning electron microscopy (SEM). Coupled to the SEM, it was used a Spectrometer Energy Dispersive (SED) Oxford INCA X-act, which was essential to evaluate the chemical composition (elements) of specific points and phase distribution of the compound.

RESULTS AND DISCUSSION

POWDER COMPOSITION

The ceramic powders (SiO_2 and $ZrSiO_4$) XRD patterns presented an additional phase (contamination) of Al_2O_3, probably from the powder processing at the supplier. This was confirmed by the XRF analysis, as seen in Table 2.

Table 2. FRX powder composition.

Material	Composition (wt.%)
Copper	99% Cu + 1% (Na, Al)
Iron	99% Fe + 1% (Si, Na, Mn, Cr, Al)
Quartz	99.5% SiO_2 + 0.5% Al_2O_3
Zirconia Silicate	97% $ZrSiO_4$ + 3% Al_2O_3
Graphite	Carbon

Table 3 demonstrates a summary on size (calculated from the Feret diameter) and morphology (shape) of each particle that constitutes the powders used as raw material.

Table 3. Characteristics of metallic and non-metallic powders.

Material	Particle size (μm)	Morphology
Copper	10 to 50	Spherical and rounded
Iron	20 to 200	Rounded and aggregate
Quartz	2 to 50	Acicular
Zirconia Silicate	2 to 40	Acicular
Graphite	10 to 100	Flake

The sequence in Fig. 3 presents the images obtained by SEM to analyze the particles size and morphology.

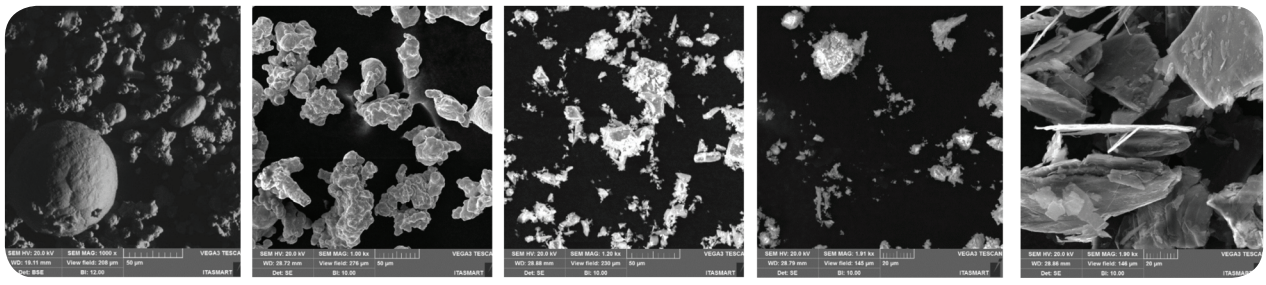

Figure 3. Particle analysis of (a) copper, (b) iron, (c) SiO_2, (d) $ZrSiO_4$, and (e) graphite.

SINTERED DENSITY

Variation of the sintered density is presented in Fig. 4. Despite a reduction in initial compaction pressure lead to significant increase in the quantity of pores, after sintering, the variation in density was significantly reduced, with the exception of the compounds I and II.

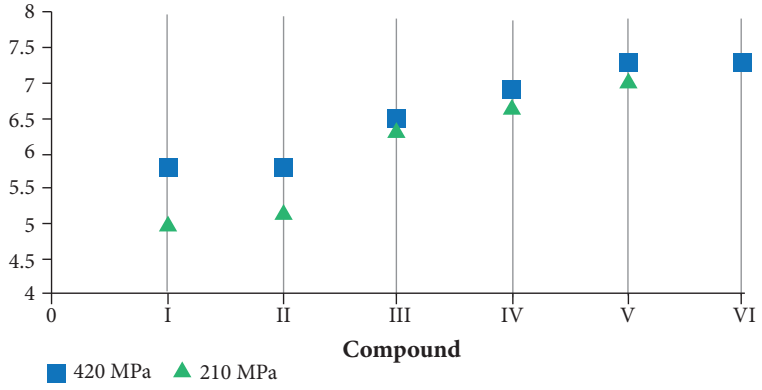

Figure 4. Sintered density.

The composition VI, which was carried out without addition of graphite, was the one with less dependence on the compaction pressure: samples pressed at 210 and 420 MPa demonstrated almost the same density after sintering. This result indicates that the graphite content affects directly the sintering process, regardless whether the compaction pressure is significantly greater. Graphite particles shear easily during mixing, thus spreading over the metallic particles, causing excessive discontinuity of the matrix and reduction in metal-metal contact (Leon *et al.* 2009). In addition, graphite is almost insoluble in copper up to very high temperatures; its solubility does not exceed 0.02% atm (Dorfman and Fuks 1995), occurring only a mechanical connection between the metal particles and graphite. This is well observed in compounds I and II microstructure, which were the ones with higher graphite content. The microstructure section explains this behavior.

MICROSTRUCTURE

Microstructure of the compounds were studied by scanning electron microscopy (SEM) with magnifications of 100 × and 250 × for general observation and 1500× for an accurate observation of the constituent's distribution in the composite material. Typical SEM micrographs are presented in Fig. 5 and Fig. 6. All images correspond to compounds pressed at 420 MPa.

The metal-metal and ceramic-metal interfacial contacts are hindered by graphite particles agglomerations, seen as the darker areas in Fig. 5.

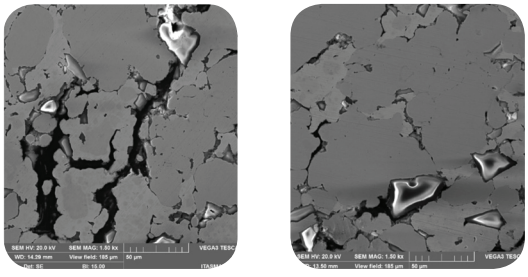

Figure 5. Microstructure of compounds I (a), and II (b).

One way to overcome this difficulty lies in the coating of graphite particles with metal (matrix) by Electroless Coating as studied by Moustafa *et al.* (2002) and Kovácik *et al.* (2008): particle contact occurs directly between metal/metal particles during

compaction and the sintering process, with the compound exhibiting behavior similar to pure metal consolidation.

In all microstructures in Fig. 6, copper appears as light gray, iron as darker gray and graphite as black. The ceramic particles are indicated in the images.

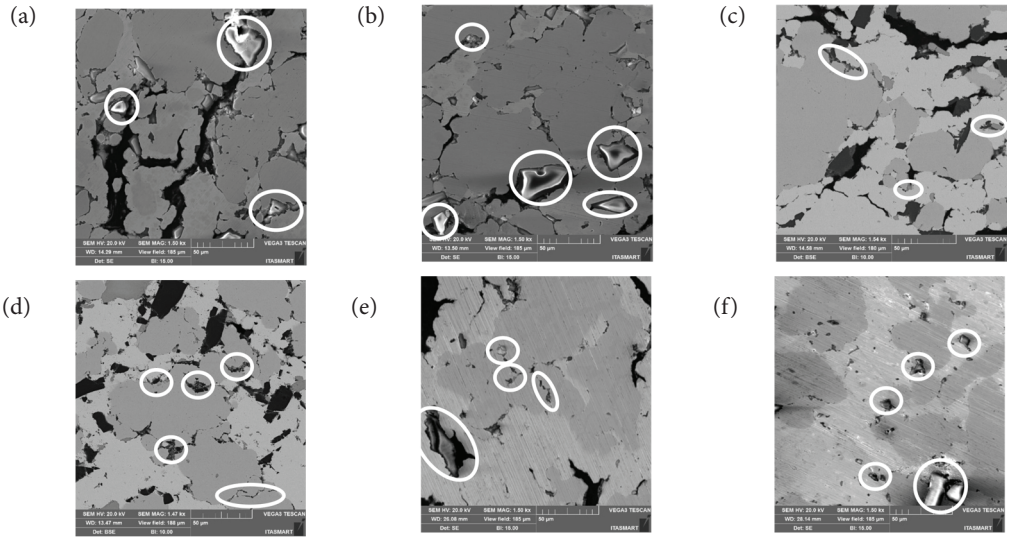

Figure 6. SEM images for a magnification of 1,500 × for compounds (a) I, (b) II, (c) III, (d) IV, (e) V, and (f) VI.

As expected, the microstructures are heterogeneous. The interfacial contact between the metal phases increased with the reduction of graphite, according to Fig. 6e. However, there was an agglomeration of ceramic particles in the Cu-Cu, Fe-Cu-Fe and Cu interface in all compounds, most likely due to the ceramic particles small grain size or some inefficiency in the mixing process.

HARDNESS

The Vickers hardness values obtained after sintering are presented in Fig. 7.

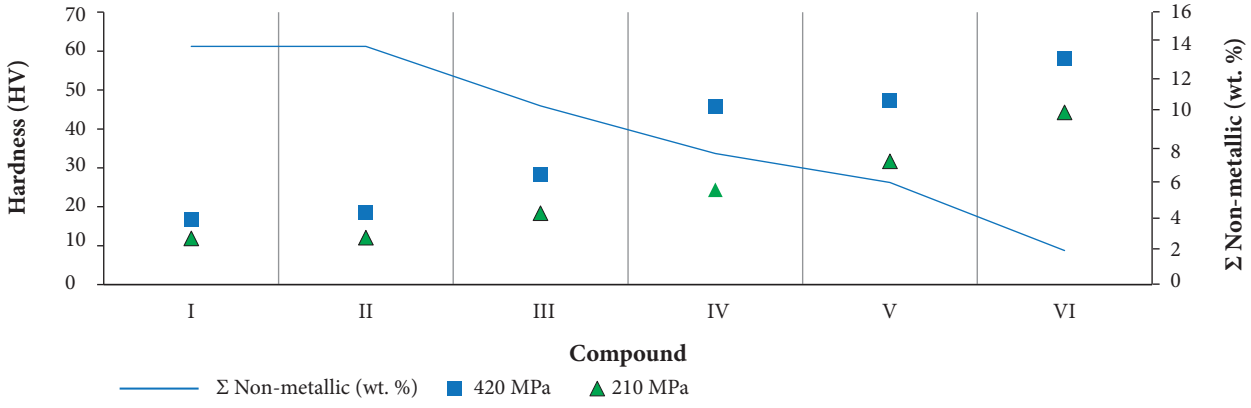

Figure 7. Vickers hardness after sintering.

The reduction of non-metallic material (graphite, SiO_2, and $ZrSiO_4$), indicated by the continuous line in Fig. 7, resulted in an increase in hardness with higher values for compaction pressure of 420 MPa. Due to a higher compaction pressure, there is an increase of the contact surface between particles, decreasing the interdiffusion distance, providing a higher densification and, consequently, increasing mechanical strength.

The compounds III and IV demonstrated a greater increase in hardness. Compounds III and IV have the same wt.% of ceramic particles, however, composition IV has four times less graphite (4 wt.% and 1 wt.%, respectively). As the hard abrasive particles provide mechanical strength to the material and the ceramic content was the same, it can be concluded that the gain in hardness was due to the graphite content. Other parameters such as sintering time and temperature, and compacting pressure, were the same.

When analyzing the friction behavior and wear mechanisms of copper matrix composites reinforced with SiC and graphite particles, Zhan and Zhang (2004) observed a decrease in mechanical properties for the composites with the increasing volume fraction of graphite particles. Moustafa *et al.* (2002) found similar results when comparing the relative density, tensile strength in compression test and Brinell hardness on composites made with Cu-coated and uncoated graphite particles. The relative density and properties obtained for compression test and the Brinell hardness are higher for the compounds of pure copper. While the samples without added graphite are deformed continuously without fracture when being compressed, the samples with added graphite suffered the fracture with an inclined angle of 45°, leading to the sample break before reaching its potential strength and ductility (brittle fracture). In addition, during compression testing, the graphite particles tend to disintegrate, which enhances the sliding mechanism and leads to the formation of pores and a brittle fracture.

SINTERING TEMPERATURE

An assessment between the Brinell hardness (diameter deformation), Vickers hardness and sintered density of compounds III (4.0 wt.% graphite – 6.5 wt.% ceramics), IV (1.0 wt.% graphite – 6.7 wt.% ceramics), and V (4.0 wt.% graphite – 2.0 wt.% ceramics) demonstrated the effect of temperature on the sintering process.

The sintering temperature was 950 °C for compositions III and IV and 1050 °C for composition V. The sintering time was the same, as well as the compaction pressure (420 MPa).

The differences in composition between samples also made it possible to evaluate the effect of graphite particles and ceramic particles in the material processing. Results are presented in Fig. 8 and Table 4. Table 4 shows, in the right column, the diameter of the deformation from the Brinell hardness test with a 10 mm steel ball and load of 500 kg.

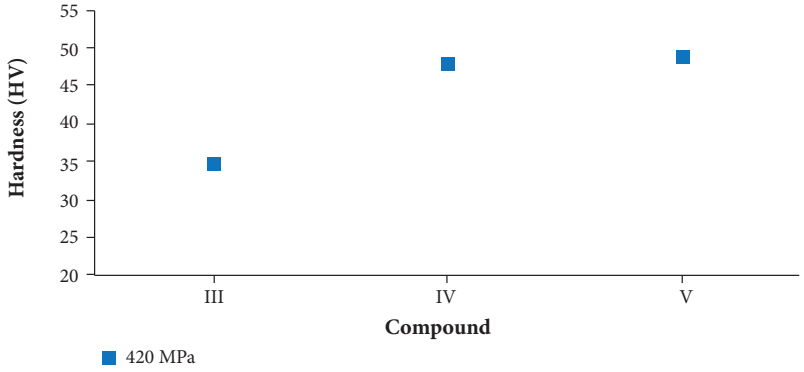

Figure 8. Vickers hardness of compounds III, IV, and V.

Table 4. Sintered density and void percentage for compounds III, IV and V.

Compound	Tsint. (°C)	Sintered Density ($g \cdot cm^{-3}$)	Voids (%)	Diameter (mm)
III	950	6.52	4.9	4.2
IV	950	6.87	6.9	3.6
V	1050	7.25	1.3	3.5

The increase in sintering temperature produced a significant reduction in pores percentage between compounds III and V (Table 4). The sintering duration required to achieve a desired degree of homogeneity is critically dependent on temperature

because interdiffusion coefficients are exponentially dependent on temperature (German 1998). Although the degree of sintering also increases with time, its effect is small compared to the temperature dependence (Upadhyaya 2000).

In addition, compound V has three times less ceramic particles (6.7 wt.% and 2 wt.%), which may produce a dual effect: an increase in sintered density and a decrease in mechanical strength (less hard particles).

Leon *et al.* (2009) analyzed the compressibility behavior of metal-ceramic powders in the preparation of copper base hybrid materials: the higher the ceramic content, the lower the densification obtained regardless of the applied method. At higher ceramic content, densification decreases, because contacts between hard particles act as shield, protecting the copper powder of being largely deformed. There is a reduction on interparticle contact and an increase in voids after hot consolidation (sintering).

Olmos *et al.* (2009) investigated the sintering behavior of metallic copper powder mixed with ceramic inclusions. The addition of inert inclusion (ceramic particles) consistently results in lower densification. It seems that most interparticles necks between copper particles in the close neighborhood of an inclusion are less developed than the necks in pure copper specimen. Additionally, pores in the neighborhood of an inclusion are noticeably larger than those inside a group of copper particles.

The deformation observed at compound III after Brinell hardness testing was significantly higher, demonstrating a lower mechanical resistance. Moreover, compound V presented Vickers hardness values about 60% higher.

Although the strength of composites that contain hard particles (ceramics) increases with the volume percentage of particles in the composite (Rohatgi *et al.* 1992), an increase in sintering temperature resulted in greater mechanical resistance, due to a higher densification.

Another aspect to be considered relates to the ceramic powder particles size (Table 3). For presenting an extremely fine grain, fine ceramic particulate agglomerations were observed in Cu-Fe, Cu-Cu and Fe-Fe interfaces (Fig. 9), which act in a harmful way in the compound consolidation during sintering.

Concerning composition IV, there was not a significant difference in Vickers hardness compared to compound V, as noted before between compounds III and V.

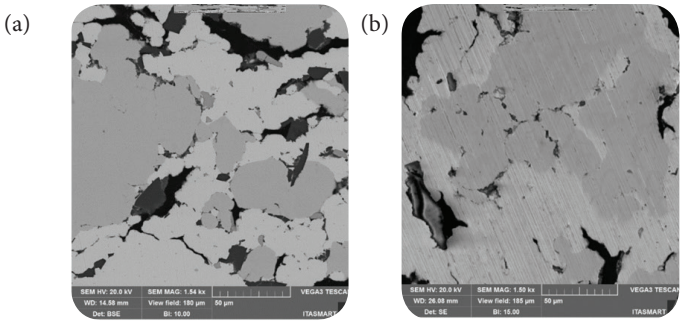

Figure 9. SEM microstructure (1500x) obtained for compounds III (a), and V (b).

The composition IV has three times more ceramic particles in relation to composition V, therefore, it would be expected a similar behavior as observed with the composition III: considerable difference in deformation after Brinell hardness testing and Vickers hardness (surface). However, composition IV was produced with four times less graphite, which greatly hinders the composite consolidation during sintering.

Furthermore, the ceramic particles provide an improvement in hardness for the compound although, at some degree, interfere with the material densification. Together with the reduced graphite content previously mentioned, this may be an explanation for the small difference between hardness values.

The effect of the sintering temperature can be observed directly by the pore percentage. The composition IV was the one that presented the greatest difference compared to compound V. Although the composition V has four times more graphite, which interferes more noticeably than ceramic particles during sintering, that was the compound with a density closer to the theoretical material density.

CONCLUSION

The graphite content affected the sintering process, regardless whether the compaction pressure is significantly greater. Its reduction (graphite) caused an increase in density by 18% and increased mechanical resistance up to 62%. The increase in compacting pressure improved mechanical strength, with more pronounced effect on the composition with a lower graphite content.

Although the strength of composites that contain hard particles (ceramics) increases with the volume percentage of particles in the composite, an increase in sintering temperature resulted in greater mechanical resistance due to a higher densification. From the microstructural analysis, it was observed that the ceramic particles hindered the sintering process by the agglomeration of ceramic inclusions in the Cu-Fe, Cu-Cu and Fe-Fe interfaces.

Increasing the sintering temperature to 1050 °C made possible the production of a compound with a moderate level of graphite (compound V) without severely affecting the material properties.

ACKNOWLEDGMENTS

The authors would like to thank Minasolo and Höganäs for providing the powders, the Instituto de Aeronáutica e Espaço, and the Instituto Tecnológico de Aeronáutica for the support.

AUTHOR'S CONTRIBUTION

Conceptualization, Santos TDES and Regiani I; Methodology, Santos TDES; Investigation, Santos TDES, Regiani I, Rocha RJ and Rocco JAFF; Writing – Original Draft, Santos TDES and Regiani I; Writing – Review & Editing, Rocha RJ and Rocco JAFF; Supervision, Rocco, JAFF.

REFERENCES

Blau PJ (2001) Compositions, functions, and testing of friction brake materials and their additives (report ORNL/TM-2001/64). Oak Ridge National Laboratory Technical Report. doi: 10.2172/788356

Cho KH, Jang H, Hong YS, Kim SJ, Bash RH, Fash JW (2008) The size effect of zircon particles on the friction characteristics of brake lining materials. Wear 264(3-4):291-297. doi: 10.1016/j.wear.2007.03.018

Dorfman S, Fuks D (1995) Carbon diffusion in copper-based metal matrix composites. Sensors and Actuators A: Physical 51(1):13-16. doi: 10.1016/0924-4247(95)01062-9

German RM (1998) Powder Metal Technologies and Applications. In: Eisen WB, Ferguson BL, German RM, Iacocca R, Lee PW, Madan D, Moyer K, Sanderow H, Trudel Y. ASM Handbook. v. 7. United States. p. 437-452.

Jang H, Kim SJ (2000) The effects of antimony trisulfide (Sb2S3) and zirconium silicate ($ZrSiO_4$) in the automotive brake friction material on friction characteristics. Wear 239(2):229-236. doi: 10.1016/S0043-1648(00)00314-8

Kim SS, Hwang HJ, Shin MW, Jang H (2011) Friction and vibration of automotive brake pads containing different abrasive particles. Wear 271(7-8):1194-1202. doi: 10.1016/j.wear.2011.05.037

Kováčik J, Emmer Š, Bielek J, Keleši L (2008) Effect of composition on friction coefficient of Cu-graphite composites. Wear 265(3-4):417-421. doi: 10.1016/j.wear.2007.11.012

Leon CA, Rodriguez-Ortiz G, Aguilar-Reyes EA (2009) Cold compaction of metal-ceramic powders in the preparation of copper base hybrid materials. Materials Science and Engineering A 526(1-2):106-112. doi: 10.1016/j.msea.2009.07.002

Liew KW, Nirmal U (2013) Frictional performance evaluation of newly designed brake pad materials. Materials and Design 48:25-33. doi: 10.1016/j.matdes.2012.07.055

Moustafa SF, El-Badry SA, Sanad AM, Kieback B (2002) Friction and wear of copper-graphite composites made with Cu-coated and uncoated graphite powders. Wear 253(7-8):699-710. doi: 10.1016/S0043-1648(02)00038-8

Nair CGK, Dutta D, Mohan G (1993) Development of metalloceramic friction material for aircraft brake. Paper presented at: ICACM 1993. Proceedings of the International Conference on Advanced Composite Materials; Wollongong, Australia.

Olmos L, Martin CL, Bouvard D (2009) Sintering of mixtures of powders: experiments and modeling. Powder Technology 190(1-2):134-140. doi: 10.1016/j.powtec.2008.04.057

Prabhu TR (2015) Airworthiness certification of Fe-Si3N4-graphite brake composites for military aircraft. Tribology in Industry, 37(4):491-499.

Rohatgi PK, Liu Y, Ray S (1992) Friction and Wear of Metal-Matrix Composites. In: Blau PJ, editor. Friction, lubrication and wear technology, ASM Handbook. v. 18. Ohio: ASM International. p. 801-811.

Shabani M, Paydar MH, Zamiri R, Goodarzi M, Moshksar MM (2016) Microstructural and sliding wear behavior of SiC-particle reinforced copper matrix composites fabricated by sintering and sinter-forging processes. J Mater Res Technol 5(1):5-12. doi: 10.1016/j.jmrt.2015.03.002

Singaravelu DL, Chandra K, Misra PS (2011) New processing technology for manufacture of heavy-duty metalloceramic brake pads. Powder Metallurgy 54(2):118-126. doi: 10.1179/174329009X409714

Upadhyaya GS (2000) Sintered metallic and ceramic materials: preparation, properties and applications. Chinchester: John Wiley & Sons Ltd.

Zhan Y, Zhang G (2004) Friction and wear behavior of copper matrix composites reinforced with SiC and graphite particles. Tribology Letters 17(1):91-98. doi: 10.1023/B:TRIL.0000017423.70725.1c